JACS
JOURNAL OF THE AMERICAN CHEMICAL SOCIETY
Article
pubs.acs.org/JACS

Circumventing Redox Chemistry: Synthesis of Transition Metal Boryl Complexes from a Boryl Nucleophile by Decarbonylation

René Frank,*[,†] James Howell,[†] Rémi Tirfoin,[†] Deepak Dange,[‡] Cameron Jones,[‡] D. Michael P. Mingos,*[,†] and Simon Aldridge*[,†]

[†]Inorganic Chemistry Laboratory, Department of Chemistry, University of Oxford, South Parks Road, Oxford OX1 3QR, United Kingdom

[‡]School of Chemistry, Monash University, PO Box 23, Melbourne, Victoria 3800, Australia

Supporting Information

ABSTRACT: The very strong reducing capabilities of the boryllithium nucleophile $(THF)_2Li\{B(NDippCH)_2\}$ (**1**, Dipp = 2,6-iPr$_2$C$_6$H$_3$) render impractical its use for the direct introduction of the $\{B(NDippCH)_2\}$ ligand via metathesis chemistry into the immediate coordination sphere of transition metals (d^n, with $n \neq 0$ or 10). Instead, **1** typically reacts with metal halide, amide and hydrocarbyl electrophiles either via electron transfer or halide abstraction. Evidence for the formation of M−B bonds is obtained only in the case of the d^5 system $[\{(HCDippN)_2B\}Mn(THF)(\mu\text{-}Br)]_2$. Lower oxidation state metal carbonyl complexes such as $Fe(CO)_5$ and $Cr(CO)_6$ react with **1** via nucleophilic attack at the carbonyl carbon atom to give boryl-functionalized Fischer carbene complexes $Fe(CO)_4\{C(OLi(THF)_3)B(NDippCH)_2\}$ and $Cr(CO)_5\{C(OLi(THF)_2)B(NDippCH)_2\}$. Although C-to-M boryl transfer does not occur for these formally anionic systems, more labile charge neutral bora-acyl derivatives of the type $L_nM\{C(O)B(NDippCH)_2\}$ [L_nM = $Mn(CO)_5$, $Re(CO)_5$, $CpFe(CO)_2$] can be synthesized, which cleanly lose CO to generate M−B bonds. From a mechanistic standpoint, an archetypal organometallic mode of reactivity, carbonyl extrusion, has thus been shown to be applicable to the boryl ligand class, with ^{13}C isotopic labeling studies confirming a dissociation/migration pathway. These proof-of-methodology synthetic studies can be extended beyond boryl complexes of the group 7 and 8 metals (for which a number of versatile synthetic routes already exist) to provide access to complexes of cobalt, which have hitherto proven only sporadically accessible.

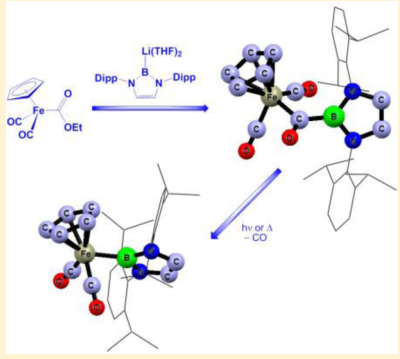

INTRODUCTION

Protocols for the introduction of a $-BX_2$ functionality into an organic molecule have received widespread recent attention, not only because the resulting C−B bonds are readily converted into C−X bonds of considerable synthetic utility (e.g., X = OH, halogen, C),[1,2] but also because certain borylation methodologies offer near-unique access to classes of feedstock for chemical synthesis (e.g., unactivated alkanes and arenes).[3−5] Transition metal boryl complexes, L_nMBX_2, have been implicated in the transfer of the boryl moiety to organic substrates via a number of routes (e.g., hydrocarbon C−H activation, hydro- and diboration of alkenes and alkynes),[6−18] and as such have been the subject of numerous studies of their structure, bonding and reactivity. That said, the relatively small number of applicable synthetic routes [typically oxidative addition of a B−X bond (X = H, hal or B), or salt metathesis utilizing a haloborane electrophile] has placed limitations on the areas of the Periodic Table from which such complexes can be accessed. As such, the vast majority of boryl systems reported to date feature a metal from the second half of the *d*-block.

The seminal discovery in 2006 of the nucleophilic lithium boryl reagents $(THF)_2Li\{B(NDippCH)_2\}$ (**1**) and its saturated counterpart $(THF)_2Li\{B(NDippCH_2)_2\}$ (Dipp = 2,6-iPr$_2$C$_6$H$_3$)[19−22] opened up synthetic routes not only for the direct borylation of organic electrophiles, but also to classes of metal boryl complex that cannot not be obtained via established routes employing boron electrophiles or B−X oxidative addition. Such examples include derivatives of *s*- and *p*-block metals/metalloids (Mg, Al, Ga, In, Tl, Si, Ge, Sn and Pb),[23−30] and *f*-block metals (Sc, Y, Gd, Er, Lu).[31,32] In most cases the boryl complexes were obtained from a boryllithium reagent and a metal halide by salt metathesis (or in the case of rare earth metal derivatives, by the reaction with cationic metal precursors).

With this in mind, and given the widespread use of alkyl/aryllithiums in similar chemistry, it is perhaps surprising that the synthesis of *d*-block metal boryl complexes from nucleophilic boryllithium reagents is currently very limited [to Ti(IV), Hf(IV), Cu(I), Ag(I), Au(I), Zn(II), Cd(II) and Hg(II) systems].[24,30,33−37] Without exception, all examples of boryl complexes containing *d*-block metals synthesized from **1** or $(THF)_2Li\{B(NDippCH_2)_2\}$ have either completely filled or empty *d*-shells (i.e., are formally d^0 or d^{10}). This obvious deficiency, and the immense potential versatility of a route to

Received: August 31, 2014
Published: October 9, 2014

dx.doi.org/10.1021/ja508979x | J. Am. Chem. Soc. 2014, 136, 15730−15741

such systems from *d*-block electrophiles, prompted us to study routes to open *d*-shell transition metal boryl complexes from boryllithium reagents.

RESULTS AND DISCUSSION

Synthetic Chemistry. In initial experiments **1** was reacted with various transition metal electrophiles (including halides, amides and organometallic complexes of the metals Mn–Ni). However, in our hands, **1** was almost invariably oxidized under such conditions to give mixtures of the hydroborane HB(NDippCH)$_2$ (presumably via a radical pathway involving hydrogen abstraction from the solvent) and haloborane XB(NDippCH)$_2$, X = Cl or Br (by metal/halide exchange).[38] The only exception to this finding is the reaction of $MnBr_2$ with **1** in THF, which generates the monoboryl species [{(HCDippN)$_2$B}Mn(THF)(μ-Br)]$_2$ (**2**) in ca. 50% yield (Scheme 1).

Scheme 1. Metathesis Reaction of Boryllithium 1 with $MnBr_2$ to Give [{(HCDippN)$_2$B}Mn(THF)(μ-Br)]$_2$ 2[a]

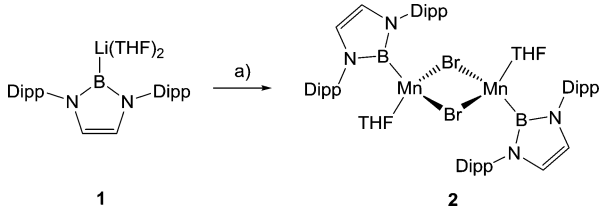

[a]Key reagents/conditions: (a) $MnBr_2$, THF, −78 to 0 °C, 5 h, 48%.

While the strongly paramagnetic nature of **2** precludes meaningful solution-phase analysis by multinuclear NMR techniques, it could be characterized unambiguously in the solid state by a combination of elemental microanalysis and X-ray crystallography (Figure 1).

It does, however, seem apparent that the strongly reducing properties of **1** mitigate against its wide-ranging effective use in metathesis chemistry. Presumably the one explicitly identified exception (Mn^{II}) is less prone to metal-centered reduction on account of its $3d^5$ configuration.[39] Thus, in the hope of achieving attenuated reactivity, the boryl anion was transmetalated onto Mg,[23] Cu and Zn[36] using established procedures. The reactions of these boryl complexes with the same library of transition metal precursors, however, also yield only hydro- or haloborane products.

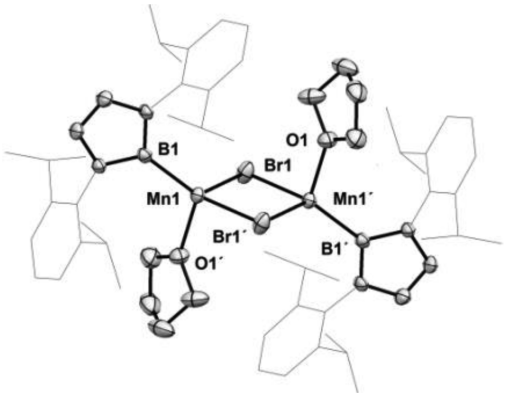

Figure 1. Molecular structure of [{(HCDippN)$_2$B}Mn(THF)(μ-Br)]$_2$ (**2**) as determined by X-ray crystallography. Thermal ellipsoids represented at the 50% level of probability; all hydrogen atoms omitted and aryl groups illustrated in wireframe format for clarity. Bond lengths (Å) and bond angles (deg): Mn1···Mn1′ 3.500(1), Mn1–Br1 2.600(1), Mn1–Br1′ 2.572(1), Mn1–B1 2.229(3), Mn1–Br1–Mn1′ 85.2(1), Br1–Mn1–Br1′ 94.8(1).

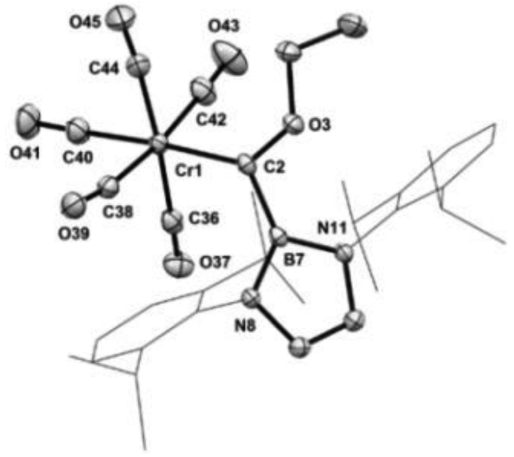

Figure 2. Molecular structure of (OC)$_5$Cr{C(OEt)B(NDippCH)$_2$}, **5**, as determined by X-ray crystallography. Thermal ellipsoids represented at the 50% level of probability; all hydrogen atoms omitted and aryl groups illustrated in wireframe format for clarity. Bond lengths (Å) and bond angles (deg): Cr1–C2 2.045(2), C2–O3 1.324(2), C2–B7 1.594(2), Cr1–C36 1.928(2), Cr1–C38 1.926(2), Cr1–C40 1.890(2), Cr1–C42 1.894(2), Cr1–C44 1.884(2), Cr1–C2–O3 130.5(1), Cr1–C2–B7 123.8(1), O3–C2–B7 105.1(1).

Since oxidation of the boryl entity by transition metal halides/amides etc. was almost invariably found to prevent M–B bond formation, metal precursors of a lower oxidation state were employed. It was hypothesized that $Fe(CO)_5$ would react with **1** via substitution of a carbonyl ligand, as has been observed for the analogous gallyl anion [Ga(NDippCH)$_2$]$^-$, which yields the anionic ferrate [Fe(CO)$_4${Ga(NDippCH)$_2$}]$^-$.[40] Our experiments, however, show that $Fe(CO)_5$ reacts with **1** in THF to give the Fischer carbene complex **3** (Scheme 2). Compound **3** can be crystallized from highly concentrated THF solutions in the presence of excess $Fe(CO)_5$. However, despite revealing a connectivity consistent with **3**, definitive X-ray crystallographic studies were frustrated

Scheme 2. Reactions of Boryllithium 1 with $Fe(CO)_5$ and $Cr(CO)_6$ to Give Boryl Fischer Carbene Complexes 3–5[a]

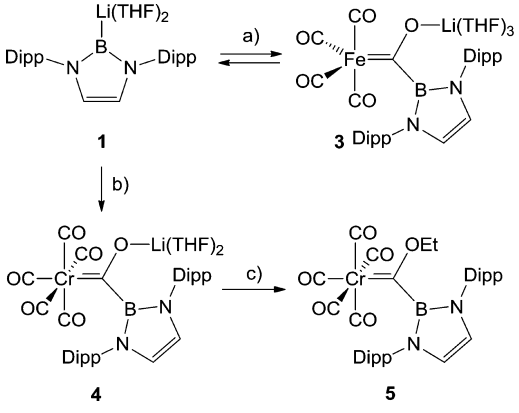

[a]Key reagents/conditions: (a) $Fe(CO)_5$, THF, room temperature; (b) $Cr(CO)_6$, THF, room temperature, 30 min; (c) [Et_3O][BF_4], dichloromethane, −78°C to room temperature, 2 h.

dx.doi.org/10.1021/ja508979x | J. Am. Chem. Soc. 2014, 136, 15730–15741

by pernicious disorder. In solution the formation of **3** is found to be reversible: in situ ^{1}H NMR monitoring (in C_6D_6) revealed a 50% reversion of **3** to the starting materials **1** and $Fe(CO)_5$ over a period of 6 h at room temperature.

In analogous fashion $Cr(CO)_6$ reacts with **1** with similar chemoselectivity to give (boryl)carbene complex **4** (Scheme 2). **4** was obtained as orange microcrystals, but, in contrast to **3**, appears to be stable to loss of the boryl moiety, and shows no signs of decomposition even in CH_2Cl_2. The constitution of **3** and **4** in general, and the number of coordinated THF molecules in particular, is based principally on NMR and IR spectroscopies together with elemental microanalysis. Each complex shows a broad signal in the respective ^{11}B{^{1}H} NMR spectrum at $\delta(^{11}B)$ = 21 ppm (cf. 45 ppm for **1**). Moreover, by analogy with traditional carbene chemistry, the alkylation of **4** could be accomplished with $[Et_3O][BF_4]$, resulting in the formation of the ethoxy(boryl)carbene complex $(OC)_5Cr\{C(OEt)B(NDippCH)_2\}$ (**5**), which could be structurally characterized in the solid state by X-ray crystallography (Figure 2), thereby providing definitive proof of composition.

On the basis of the chemistry outlined in Scheme 2, it was concluded that simple metal carbonyl complexes are unlikely to provide access to M−B bonds via reactions with boryllithium reagents. The preference for nucleophilic attack at a ligand-centered electrophilic site contrasts with the substitution chemistry observed for analogous gallyl nucleophiles, but does have precedent in the reactivity of the same boryl/gallyl reagents toward titanium pyridine complexes.[41] That said, what the syntheses of (boryl)carbene complexes **3** and **4** do at least demonstrate is that the incorporation of the boryl entity, $\{B(NDippCH)_2\}$, into the overall ligand sphere of a transition metal complex can be achieved using a boron-centered nucleophile.

In simple valence bond terms, the structure of complex **4** can be described in terms of two limiting resonance structures (Scheme 3). One of these (bora-acyl **4b**) suggests parallels with

Scheme 3. Limiting Resonance Structures for the Anionic Component of 4: (Boryl)Carbene 4a and Bora-Acyl 4b

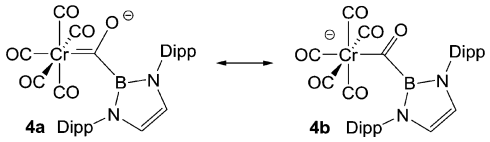

classical carbon-based acyl chemistry, for which insertion/deinsertion of carbon monoxide into/from metal−carbon bonds is known to be facile (typically via a dissociation/migration mechanism).[42] In the case of **4**, carbon monoxide extrusion does not occur, presumably due to its anionic nature, and the consequently high degree of back-bonding from chromium to the carbonyl ligands. We hypothesized, however, that the isoelectronic (charge neutral) manganese species $(OC)_5Mn\{C(O)B(NDippCH)_2\}$ should be more amenable to spontaneous loss of CO and subsequent rearrangement to form a M−B bond.

With this in mind, a suitable precursor for the manganese bora-acyl complex $(OC)_5Mn\{C(O)B(NDippCH)_2\}$ was sought. Previous studies of the chemistry of **1** are consistent with high yielding nucleophilic reactivity toward organic carbonyl compounds. Thus, PhC(O)X (X = Cl, OPh, OC(O)Ph), $[t\text{BuOC(O)}]_2O$ and $(PhO)_2C(O)$ react cleanly to give the boryl ketone $PhC(O)B(NDippCH)_2$, or the boryl esters $t\text{BuOC(O)B(NDippCH)}_2$ and $PhO(O)CB(NDippCH)_2$, respectively.[20] On this basis, we reasoned that an *organometallic* ester, e.g., $(OC)_5Mn\{C(O)OEt\}$ **6**, might react with **1** to produce the desired metal bora-acyl complex (e.g., **7**), which could then rearrange to give a boryl complex (i.e., **8**; Scheme 4).

Scheme 4. Reaction of Boryllithium 1 with Manganese Ester 6 to Give Boryl Complex 8[a]

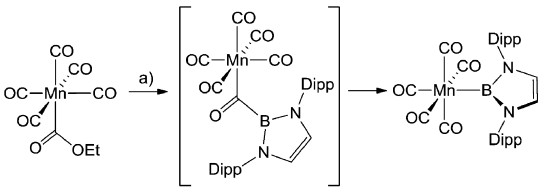

[a]Key reagents/conditions: (a) **1**, THF, room temperature, 30 min.

In the event, the reaction of **1** with **6** generates manganese boryl complex $(OC)_5Mn\{B(NDippCH)_2\}$ (**8**) directly. Compound **8** is stable in air, and could be purified by column chromatography. Subsequent solvent evaporation from a solution in hexanes affords colorless crystals suitable for X-ray crystallography, thereby providing definitive structural characterization in the solid state (Figure 3). At no point was any

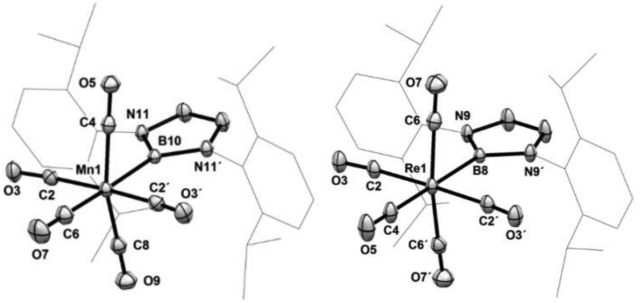

Figure 3. (left to right) Molecular structures of $(OC)_5M\{B(NDippCH)_2\}$ (**8**: M = Mn; **11**: M = Re) as determined by X-ray crystallography. Thermal ellipsoids represented at the 50% level of probability; all hydrogen atoms omitted and aryl groups illustrated in wireframe format for clarity. Bond lengths (Å) and bond angles (deg): (for **8**) Mn1−B10 2.178(2), Mn1−C2 1.860(1), Mn1−C4 1.833(2), Mn1−C6 1.843(2), Mn1−C8 1.840(2), C2−Mn1−B10 93.3(1), C4−Mn1−B10 of 75.8(1), C8−Mn1−B10 83.3(1)°; (for **11**) Re1−B8 2.292(4), Re1−C2 2.018(3), Re1−C4 1.977(4), Re1−C6 1.994(3), C2−Re1−B8 91.7(1), C6−Re1−B8 83.8(1).

explicit evidence obtained for the bora-acyl intermediate **7**, even in ^{1}H and ^{11}B{^{1}H} NMR measurements carried out at −40 °C. Thus, in order to obtain further mechanistic information, we targeted the rhenium analogue of **7**, which we hypothesized would be less labile than its 3*d*-metal counterpart.

The reaction of **1** with the related rhenium ester $(OC)_5Re\{C(O)OMe\}$ **9** does indeed generate an isolable bora-acyl species [viz. $(OC)_5Re\{C(O)B(NDippCH)_2\}$, **10**; Scheme 5] in ca. 90% yield (by NMR) after extraction of the crude product into hexanes. For structural verification, orange crystals of **10** suitable for X-ray crystallography could also be obtained by solvent evaporation from a solution in hexanes (Figure 4). Compound **10** is stable as a solid (even in air) but in solution is

dx.doi.org/10.1021/ja508979x | J. Am. Chem. Soc. 2014, 136, 15730−15741

Scheme 5. Reaction of Boryllithium 1 with Rhenium Ester 9 to Give Bora-Acyl Complex 10; Subsequent Rearrangement at Ambient Temperature to Give Boryl Complex 11 via Liberation of Carbon Monoxide[a]

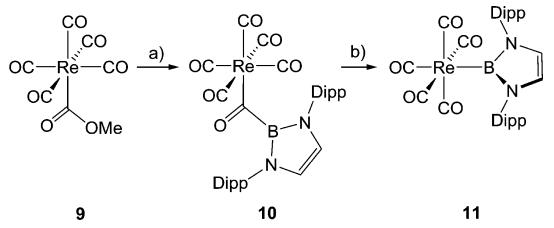

[a]Key reagents/conditions: (a) **1**, THF, room temperature, 30 min; (b) THF, 40°C, 2 d.

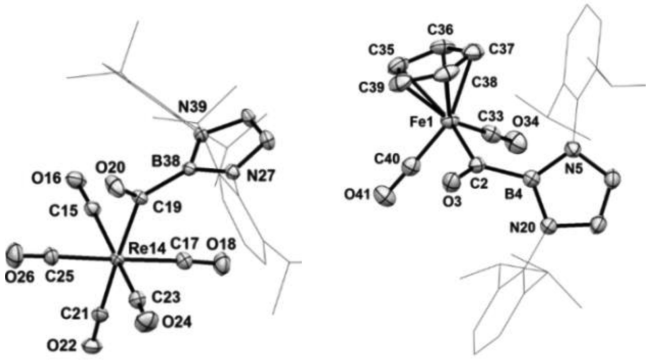

Figure 4. (left to right) Molecular structures of $(OC)_5Re\{C(O)B(NDippCH)_2\}$, **10** (only one molecule of the asymmetric unit is illustrated), and $CpFe(CO)_2\{C(O)B(NDippCH)_2\}$, **13**, as determined by X-ray crystallography. Thermal ellipsoids represented at the 50% level of probability; all hydrogen atoms omitted and aryl groups illustrated in wireframe format for clarity. Bond lengths (Å) and bond angles (deg): (for **10**) Re14–C19 2.239(3), C19–O20 1.224(4), C19–B38 1.596(4); in the carbonyl ligands the bond lengths cover the ranges for Re–C [197.9(4)–202.5(3)] and C–O [112.3(4)–115.3(5)]; (for **13**) Fe1–C2 2.008(2), C2–O3 1.217(2), C2–B4 1.589(2), Fe1–C35 2.127(2), Fe1–C36 2.138(2), Fe1–C37 2.122(2), Fe1–C38 2.120(2), Fe1–C39 2.105(2), Fe1–C33 1.760(2), Fe1–C40 1.753(2), C33–O34 1.153(2), C40–O41 1.152(2), Fe1–C2–O3 119.9(1), Fe1–C2–B4 120.5(1), O3–C2–B4 119.7(2).

converted slowly into a second boron-containing species (for example over 7 days at ambient temperature in C_6D_6). In situ $^{11}B\{^1H\}$ NMR monitoring shows conversion of the signal for **10** [$\delta(^{11}B)$ = 23 ppm] to a resonance at 33 ppm, together with a minor signal at 19 ppm. Column chromatography enables the isolation of the former species as a single substance, and subsequent crystallization from hexanes by slow solvent evaporation yields colorless crystals of the air-stable rhenium boryl complex $(OC)_5Re\{B(NDippCH)_2\}$ (**11**) suitable for X-ray crystallography (Figure 3).

Both rhenium bora-acyl complex **10** and its putative manganese analogue **7** are labile at temperatures close to ambient, presumably as a result of the carbonyl-only ancillary ligand set. In order to investigate further the chemistry of the novel bora-acyl ligand and, in particular, its propensity to undergo carbonyl extrusion, we therefore targeted more electron-rich metal systems, reasoning that (if CO ligand loss were important mechanistically) such systems would face a substantially higher barrier to this onward reaction. Thus, we targeted analogous complexes featuring a π-donor ancillary ligand such as cyclopentadienyl (Cp). Accordingly, the reaction of **1** with the half-sandwich ester $CpFe(CO)_2\{C(O)OEt\}$ (**12**) gives the acyl species $CpFe(CO)_2\{C(O)B(NDippCH)_2\}$ **13** in 95% conversion by $^{11}B\{^1H\}$ NMR spectroscopy [$\delta(^{11}B)$ = 19 ppm; Scheme 6].

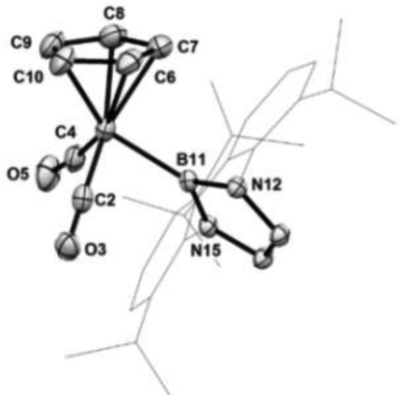

Figure 5. Molecular structure of $CpFe(CO)_2\{B(NDippCH)_2\}$ (**14**) as determined by X-ray crystallography. Thermal ellipsoids represented at the 50% level of probability; all hydrogen atoms omitted and aryl groups illustrated in wireframe format for clarity. Bond lengths (Å) and bond angles (deg): Fe1–B11 2.052(2), Fe–C2 1.743(2), Fe1–C7 1.755(2), Fe1–C6 2.106(2), Fe1–C7 2.099(2), Fe1–C8 2.093(2), Fe1–C9 2.109(2), Fe1–C10 2.111(2), C2–Fe1–C4 91.3(1), C2–Fe1–B11 78.7(1), C4–Fe1–B11 96.8(1).

Scheme 6. Reaction of Boryllithium 1 with Iron Ester 12 Yielding the Stable Bora-Acyl Species 13; Subsequent Rearrangement under Forcing Conditions to Give Boryl Complex 14 with Liberation of Carbon Monoxide[a]

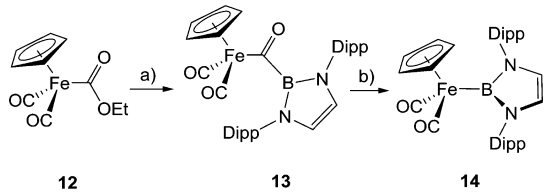

[a]Key reagents/conditions: (a) **1**, THF, room temperature, 30 min; (b) *m*-xylene, 140°C, 12 h or $h\nu$, 30 min.

In contrast to rhenium bora-acyl complex **10**, **13** is kinetically inert in solution at/close to room temperature. It is also air stable, and column chromatography can be exploited to yield analytically pure samples; orange crystals suitable for X-ray crystallography could subsequently be grown by slow solvent evaporation from a solution in hexanes (Figure 4). As anticipated, **13** is found to be robust with respect to decarbonylation, which requires forcing conditions (heating to 140 °C or UV photolysis) in order to generate boryl complex **14**. The rearrangement process is conveniently monitored through the signals in the $^{11}B\{^1H\}$ NMR spectrum [$\delta(^{11}B)$ = 19 ppm for **13** to $\delta(^{11}B)$ = 36 ppm for **14**]. As in the cases of boryl complexes **8** (manganese) and **11** (rhenium), **14** is stable in air, and could be purified by column chromatography. Structural verification by X-ray crystallography was possible using yellow crystals obtained by slow solvent evaporation from a hexane solution (Figure 5).

By contrast, the analogous iron thioester $CpFe(CO)_2\{C(S)OMe\}$ **15** reacts under similar conditions to yield thiocarbonyl complex $CpFe(CO)(CS)\{C(O)B(NDippCH)_2\}$ (**16**; Scheme

dx.doi.org/10.1021/ja508979x | J. Am. Chem. Soc. 2014, 136, 15730–15741

Scheme 7. Reaction of Boryllithium 1 with Iron Thioester 15 Yielding the Thiocarbonyl Ligated Bora-Acyl Species 16[a]

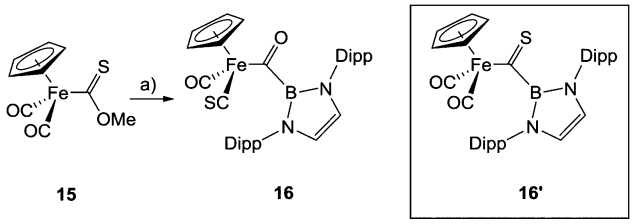

[a]Key reagents/conditions: (a) **1**, THF, room temperature, 5 min.

7), rather than a product containing the C(S)(boryl) unit [i.e., $CpFe(CO)_2\{C(S)B(NDippCH)_2\}$, **16**′]. Compound **16** was obtained as orange crystals suitable for X-ray crystallography from hexanes after appropriate workup (Figure 6).

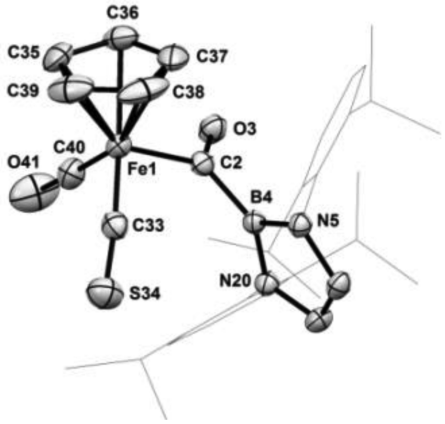

Figure 6. Molecular structure of $CpFe(CO)_2\{C(O)B(NDippCH)_2\}$, **16**, as determined by X-ray crystallography. Thermal ellipsoids represented at the 50% level of probability; lattice solvent (*n*-hexane) and all hydrogen atoms omitted; aryl groups illustrated in wireframe format for clarity. Bond lengths (Å): Fe1−C2 2.004(2), Fe1−C33 1.734(2), Fe1−C40 1.754(2), C40−O41 1.241(3), C33−S34 1.523(2), C2−O3 1.241(3), C2−B4 1.587(3).

The formation of **16** could conceivably occur via rearrangement of **16**′ [itself formed by initial boryl attack at the C(S)OMe ligand] with the isomerization driven by the generation of the stronger acyl C═O bond and the increased π acceptor properties of the CS ligand (over CO). However, we observe no explicit spectroscopic evidence for **16**′ as an intermediate species. Another possibility (Scheme 8) is that **16** results from direct attack by **1** at one of the terminal carbonyl ligands of **15** to give a Fischer carbene complex in a fashion directly analogous to the syntheses of **3** and **4** (Scheme 2), which then rearranges to yield **16**. This mechanistic alternative (and the possibility of a similar process occurring in the reaction of **1** with **12**) prompted us to examine in greater depth the formation of **13** from **12**, by the use of ^{13}C isotopic labeling.

The doubly ^{13}CO-labeled isotopomer of **12** [$CpFe(^{13}CO)_2\{C(O)OEt\}$, **12**-$^{13}C_2$] was prepared from $Na[CpFe(^{13}CO)_2]$ and ClC(O)OEt (Scheme 9). Although **12**-$^{13}C_2$ is isotopically labile (with scrambling of ^{13}C to give a statistical mixture of carbonyl and acyl labeled systems occurring over ca. 4 h at room temperature), freshly prepared samples (or those generated in situ) can be reacted with **1** in THF to cleanly generate **13**-$^{13}C_2$, which does not undergo analogous

Scheme 8. Possible Mechanisms for the Formation of Bora-Acyl Species from the Corresponding Ester via Either Direct Attack at the Ester Function (Red), or Initial Attack at a Carbonyl Ligand to Give a Borylated Fischer Carbene Intermediate (Blue)[a]

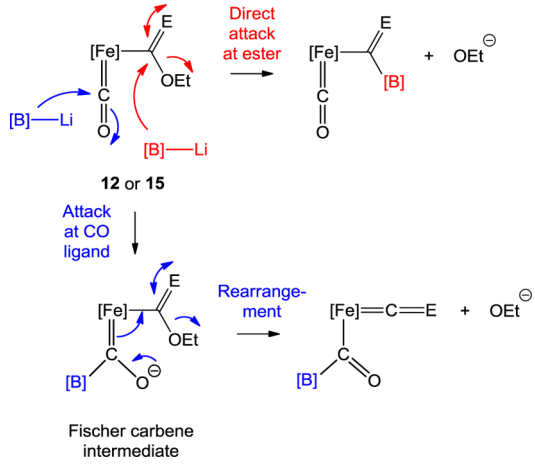

[a][Fe] = CpFe(CO), E = O or S, [B] = $B(NDippCH)_2$, Li = $Li(THF)_2$.

Scheme 9. ^{13}C Labeling Studies of the Formation of 14 from 12[a]

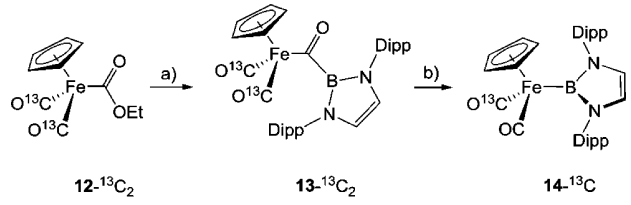

[a]Key reagents/conditions: (a) **1**, THF, room temperature, 30 min; (b) *m*-xylene, 140°C, 12 h or $h\nu$, 30 min.

scrambling. Clear indication for the formation of **13**-$^{13}C_2$ as $CpFe(^{13}CO)_2\{C(O)B(NDippCH)_2\}$ instead of the alternative product $CpFe(^{13}CO)(CO)\{^{13}C(O)B(NDippCH)_2\}$ is obtained by IR spectroscopy. This observation implies a mechanism proceeding via direct attack of **1** at the ester function of **12** rather than at a carbonyl ligand. Moreover, the product **13**-$^{13}C_2$ can subsequently be subjected to rearrangement conditions (either thermal or photolytic) and in both cases yields the monolabeled complex **14**-^{13}C as the only detectable product. Thus, the rearrangement of the bora-acyl unit to a boryl complex appears to follow the classic organometallic pathway, i.e., via loss of a carbonyl ligand from the metal prior to migration.[42]

Boryl complexes of manganese, rhenium and iron have, of course, been reported previously;[43] examples include the catecholboryl systems $(OC)_5Mn(Bcat)$ (**17**, cat = 1,2-$O_2C_6H_4$), $(OC)_5Re(Bcat)$ (**18**), and $CpFe(CO)_2(Bcat)$ (**19**),[4,5,44] which can be prepared by the reaction of the respective anionic metallates with boron electrophiles such as ClBcat. However, in our hands, this synthetic route is demonstrably ineffective using the bromoborane $BrB(NDippCH)_2$, presumably due to both the steric demands of the bulky Dipp-substituted ligand backbone, and the lower electrophilicity of a di*amino*haloborane precursor. Moreover, this methodology also fails for cobalt with *any* haloborane electrophile. Early syntheses reported using this approach

dx.doi.org/10.1021/ja508979x | J. Am. Chem. Soc. 2014, 136, 15730−15741

purporting to yield cobalt boryl complexes[45,46] lack experimental and analytical details and have subsequently been called into question.[47,48] Indeed, in our hands, the reactions of $Na[Co(CO)_4]$ with boranes of the type Ar_2BX in toluene do not yield the reported $(OC)_4CoBAr_2$ compounds,[45] but rather boryloxycarbyne complexes of the type $\{(OC)_3Co\}_3(\mu_3\text{-}COBAr_2)$ (Scheme 10). Thus, with Mes_2BBr (Mes = 2,4,6-

Scheme 10. Reaction of Mes_2BBr with $Na[Co(CO)_4]$ Yielding the Trinuclear Cobalt Carbyne Cluster 20[a]

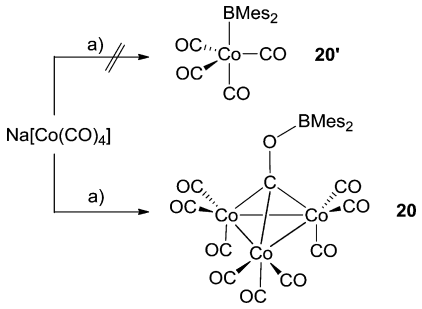

[a]Key reagents/conditions: (a) Mes_2BBr, toluene, 45°C, 4 d. Mes = 2,4,6-$Me_3C_6H_2$.

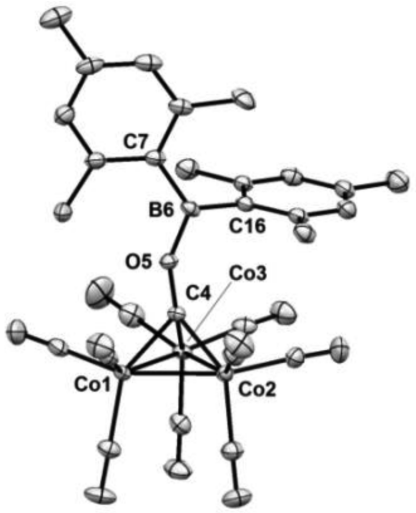

Figure 7. Molecular structure of $\{(OC)_3Co\}_3(\mu_3\text{-}COBMes_2)$, **20**, as determined by X-ray crystallography. Thermal ellipsoids represented at the 50% level of probability; all hydrogen atoms omitted. Bond lengths (Å) and bond angles (deg): Co1−Co2 2.4602(6), Co2−Co3 2.4788(6), Co1−Co3 2.4710(6), Co1−C4, 1.929(3), Co2−C4 1.910(3), Co3−C4 1.894(3), C4−O5 1.338(3), O5−B6 1.394(4), C4−O5−B6 135.7(2).

$Me_3C_6H_2$) compound **20** was obtained as deep purple crystals which were suitable for X-ray crystallography (Figure 7). The formation of **20** instead of **20′** may be attributed to the higher nucleophilicity of the carbonyl oxygen atoms compared to cobalt itself, presumably due to the contracted nature of the *d*-orbitals associated with a later transition metal center. As such, fully characterized (and structurally authenticated) cobalt boryl complexes comprise only three examples, synthesized in most cases from a diboron(IV) reagent (i.e., B_2cat_2 or B_2pin_2; pin = $O_2C_2Me_4$).[49−52]

In view of the paucity of versatile synthetic routes to cobalt boryl systems and the importance of the corresponding complexes of the heavier congeners rhodium/iridium in

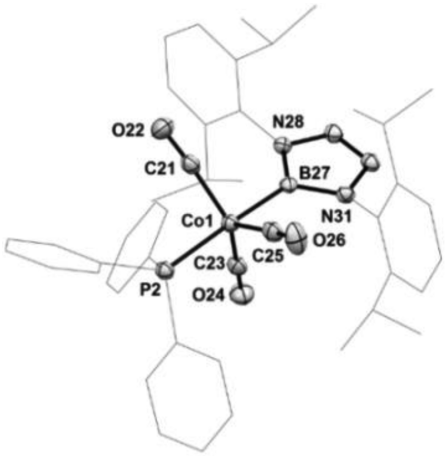

Figure 8. Molecular structure of $(Ph_3P)(OC)_3Co\{B(NDippCH)_2\}$, **22**, as determined by X-ray crystallography. Thermal ellipsoids represented at the 50% level of probability; all hydrogen atoms omitted and aryl groups illustrated in wireframe format for clarity. Bond lengths (Å) and bond angles (deg): Co1−B27 2.058(3), Co1−P1 2.2184(8), Co1−C21 1.774(3), Co1−C23 1.762(3), Co1−C25 1.785(3), C21−O22 1.142(4), C23−O24 1.149(4), C25−O26 1.138(4), B27−Co1−C23 78.35(13).

numerous borylation methodologies, we targeted an extension of our new methodology to cobalt systems. Accordingly, the reaction of the cobalt ester **21** with **1** was probed in THF solution. Consistent with the results obtained for the related $[Mn(CO)_5]$ system, cobalt boryl complex **22** is obtained without any direct observation of a putative bora-acyl intermediate (Scheme 11). Here too, the boryl product was

Scheme 11. Reaction of Boryllithium 1 with Cobalt Ester 21 to Give Boryl Complex 22[a]

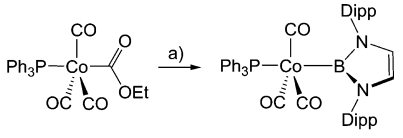

[a]Key reagents/conditions: (a) **1**, THF, −35°C for 6 h then room temperature for 24 h.

found to be stable in air, and bulk samples could be obtained via column chromatography with analytical purity. **22** is characterized by $^{11}B\{^1H\}$ and $^{31}P\{^1H\}$ NMR signals at 32 and 51.7 ppm, respectively, by two methyl/one methine signal for the Dipp substituents in the ^1H NMR spectrum and by IR-measured carbonyl stretches at 2026, 1962, and 1928 cm^{-1}. Slow solvent evaporation from a solution in hexanes gives colorless crystals suitable for X-ray crystallography (Figure 8). A range of cobalt ester derivatives are available in the current literature and, as such, this new synthetic route offers potential access to a systematic study of cobalt boryl complexes.[53,54]

Structural Studies. Most new compounds synthesized during the course of this study proved to be amenable to structural study in the solid state by X-ray crystallography. Among these, compound **5** represents, to our knowledge, the first boryl derivatized Fischer carbene complex (although "free" boryl-substituted carbenes and their heavier Group 14 analogues have been reported).[29,55] With respect to the

dx.doi.org/10.1021/ja508979x | J. Am. Chem. Soc. 2014, 136, 15730−15741

metal-carbene interaction, the bonding situation appears to be comparable to known, structurally characterized, alkyl or aryl substituted Fischer carbene complexes such as $Cr(CO)_5\{C(OEt)Me\}$[56] and $Cr(CO)_5\{C(OMe)Ph\}$.[57] Thus, the Cr−$C_{carbene}$ and *trans* Cr−C(O) distances [2.045(2) and 1.890(2) Å; Figure 2] are very similar to those determined for $Cr(CO)_5\{C(OEt)Me\}$ [2.053(6) and 1.893(5) Å, respectively].[56] The carbonyl stretching frequency for the ligand *trans* to the carbene is slightly higher for alkyl/aryl substituted carbene complexes as can be seen in the series $Cr(CO)_5\{C(OEt)R\}$ for R = Me, Ph and $B(NDippCH)_2$ [ν(CO) = 2064, 2062, 2056 cm^{-1}].[58]

Although boryl complexes of the group 7 and 8 metals have been reported previously, such systems have not typically been reported in association with "non-organometallic" supporting ligand sets such as that found in $[\{(HCDippN)_2B\}Mn(THF)(\mu\text{-Br})]_2$ (**2**). Indeed, the overall dimeric structure of **2** (Figure 1) is more reminiscent of aryl and amido systems of the type $[XM(THF)(\mu\text{-hal})]_2$ (X = bulky terphenyl or amido group).[59,60] Thus, the Mn···Mn and Mn−Br distances [3.500(1) and 2.600(1)/2.572(1) Å], and the angles within the planar Mn_2Br_2 ring [94.8(1)° at Mn(1), 85.2(1)° at Br(1)] are very similar to those reported for $[\{(Dipp^*)(Me_3Si)N\}Mn(THF)(\mu\text{-Br})]_2$ [3.574(1) and 2.597(1)/2.579(1) Å; 92.7(1) and 87.3(1)°; Dipp* = C_6H_2-4-Me-2,6-$(CHPh_2)_2$].[60] The Mn−B distance [2.229(3) Å] is somewhat longer than that found in Mn^I boryl complex **8**, [2.178(2) Å], a phenomenon which (given the smaller size of Mn^{II}) is at least partly steric in origins. The Evans method determined magnetic moment for **2** in C_6D_6 [6.8(2) BM], while less than the spin-only value (8.36 μ_B), is consistent with retention of the dimeric structure in solution, if allowance is made for similar antiferromagnetic Mn/Mn coupling as observed for related amido systems.[60]

For the novel boryl complexes of manganese, rhenium and iron carbonyls (**8**, **11** and **14**; Figures 3 and 5) key spectroscopic/structural parameters can be compared with the corresponding data for the catecholboryl systems $(OC)_5Mn(Bcat)$ (**17**), $(OC)_5Re(Bcat)$ (**18**) and $CpFe(CO)_2(Bcat)$ (**19**) (Table 1).[4,44] Notably, the metal−boron bond lengths measured for complexes **8**, **11** and **14** are longer than those of the corresponding catecholboryl compounds **17**−**19**. Moreover, the respective IR spectra show that complexes **8**, **11** and **14** give rise to significantly lower wavenumber carbonyl stretching vibrations than their catecholboryl analogues. While the former observation almost certainly reflects the greater steric demands of the $B(NDippCH)_2$ ligand (over Bcat), longer M−B bonds are also consistent with the greater *trans*-influence of diamino- vs diaryloxoboryl ligands demonstrated by Lin and Marder.[61] The presence of NR_2, rather than OR substituents at boron is thought to lead to greater B 2p character (and lower B 2s character) in the σ-donor orbital of the boryl ligand, which is responsible not only for greater σ-donor strength (higher HOMO energy), but also for the longer M−B bond. These factors (together with the steric shielding of the M−B bond by the peripheral aryl substituents) may also underpin differences in chemical behavior: **17**−**19** are prone to hydrolysis, but **8**, **11** and **14** are stable in air and even tolerate chromatographic purification.

Table 1. Comparison of Structural and Spectroscopic Data for the Boryl Complexes $(OC)_5Mn\{B(NDippCH)_2\}$ (8), $(OC)_5Mn(Bcat)$ (17), $(OC)_5Re\{B(NDippCH)_2\}$ (11), $(OC)_5Re(Bcat)$ (18), $CpFe(CO)_2\{B(NDippCH)_2\}$ (14) and $CpFe(CO)_2(Bcat)$ (19)

metal	compound	d(M−B)/Å	$\delta(^{11}B)$/ppm	$\nu(CO)^{a,b}$/cm^{-1}	ref.
Mn	**8**	2.178(2)	34	1976	this work
Mn	**17**	2.108(6)	49	2009	4
Re	**11**	2.292(4)	33	1970	this work
Re	**18**	[c]	44	2016	4
Fe	**14**	2.052(2)	36	1992, 1931	this work
Fe	**19**	1.959(6)	52	2024, 1971	44

[a]For complexes of the $M(CO)_5$-type, the stretching vibration of the axial carbonyl ligand is stated. [b]IR data (including those for reference compounds) obtained from KBr disks. [c]Structural data not available for **18**.

Postulated acyl intermediate **7**, together with its less labile counterparts **10** and **13** (Figure 4) can be considered as an analogue of classical metal acyl compounds. In the cases of **10** and **13** these represent the first examples containing three-coordinate boron as part of a metal-acyl entity. At first sight, the apparently low activation barriers via which **7** and **10** decarbonylate is somewhat surprising, given that related carbon-based acyl compounds of the types $(OC)_5Mn\{C(O)R\}$ and $(OC)_5Re\{C(O)R\}$ (R = Me or Ph) are stable at ambient temperature and require heating or UV-photolysis to rearrange.[62,63] In the IR spectra of both **10** and **13**, the C═O stretching vibration for the acyl group falls in a range similar to known benzoyl complexes, but lower than the respective acetyl compounds (Table 2). Moreover, the metal-bound carbonyl ligands in **10** and **13** vibrate at similar wavenumber to the related carbon based acyl compounds. These data therefore give relatively little indication that the relative lability of **7**/**10** is due to electronic factors. On the other hand, for a reaction involving carbonyl dissociation prior to boryl migration (as shown explicitly for the related iron system **13** by ^{13}C isotopic labeling), the increased steric bulk of the boryl substituent (over Me or Ph-containing acyl systems) might be expected to lead to a lower activation barrier if CO loss were rate-determining.

The related thiocarbonyl complex **16** is unstable in solution, but crystals of appropriate quality for X-ray crystallography could rapidly be grown from hexanes at −35 °C (Figure 6). The lower stability of **16** compared to **13** can potentially be related to stronger back-bonding to the thiocarbonyl unit, and a consequently weaker interaction (and greater lability) associated with the single CO ligand. This notion is consistent with the observation of a shorter Fe−CS bond length Fe1−C33 [1.734(2) Å] compared to the Fe−CO bond lengths in **13** and **16** [1.753(2)−1.760(2) Å].

Complex **22** is the first carbonyl containing cobalt boryl complex (Figure 8). Since the number of cobalt boryl compounds is extremely limited, **22** may perhaps best be compared with the related $[L_4Co]$ complex $(Me_3P)_4CoBcat$.[51] Here too, in accordance with the higher p character of the σ-donor orbital of the boryl ligand, the Co−B bond length is longer in **22** than the Bcat complex [2.058(3) vs 1.949(2) Å]. Trimetallic boryloxycarbyne system **20** (Figure 7) finds precedent in iron and nickel systems reported by Braunschweig and co-workers.[66]

CONCLUSIONS

The very strong reducing capabilities of boryllithium complex **1** render impractical its use for the systematic introduction of the $\{B(NDippCH)_2\}$ ligand via metathesis chemistry into the

Table 2. Comparison of the CO Stretching Vibrational Modes of Carbon Based Acyl Complexes with the Boryl Substituted Acyl Complexes Obtained in This Work

	wavenumber/cm^{-1}[a]		
compound	R = Me	R = Ph	R = B(NDippCH)$_2$
(OC)$_5$Re{C(O)R}	1975 (axial CO)	1981 (axial CO)	1973 (axial CO)
	1601 (acyl)[63]	1562 (acyl)[63]	1563 (acyl)
CpFe(CO)$_2${C(O)R}	2018, 1963	2029, 1972	2001, 1940
	1655 (acyl)[64]	1603 (acyl)[65]	1610 (acyl)

[a]IR data (including those for reference compounds) obtained from KBr disks.

immediate coordination sphere of transition metals (d^n, with $n \neq 0$ or 10). In our hands, **1** appears to react with metal halide, amide and hydrocarbyl electrophiles via either electron transfer or halide abstraction, with evidence being accrued for the formation of M−B bonds only in the case of the d^5 system [{(HCDippN)$_2$B}Mn(THF)(μ-Br)]$_2$. Metal carbonyl complexes such as Fe(CO)$_5$ and Cr(CO)$_6$ react with **1** via nucleophilic attack at the carbonyl carbon atom to give boryl-functionalized Fischer carbene complexes. While subsequent C-to-M boryl transfer does not occur for these formally anionic systems, related charge neutral bora-acyl derivatives cleanly lose CO to generate M−B bonds. Such an approach can be used not only in proof-of-methodology studies to synthesize boryl complexes of group 7 and 8 metals (for which a number of versatile synthetic routes already exist), but also to provide access to boryl compounds of cobalt, which have hitherto proven only sporadically accessible. With this new synthetic route now in hand, we are currently investigating the reactivity of cobalt boryl systems toward C═C and C−H bonds, with a view to offering systematic comparison with the corresponding chemistry enabled by the noble metals rhodium and iridium.

From a mechanistic standpoint, an archetypal organometallic mode of reactivity, carbonyl extrusion, has been shown to be additionally applicable to the boryl ligand class. However, while the facile insertion of CO into M−Me and M−Ph bonds demonstrates the reversibility of carbon monoxide deinsertion for metal acyls, the corresponding chemistry for bora-acyl complexes is found to be irreversible. Thus, even under forcing conditions, or in the presence of a strong Lewis acid such as AlBr$_3$, no evidence is seen for the assimilation of CO by the M{B(NDippCH)$_2$} function to generate M{C(O)B(NDippCH)$_2$}. Such observations are consistent with DFT calculations on the model systems (OC)$_5$Mn{C(O)X} {X = Me, B(NMeCH)$_2$} which show that the decarbonylation reaction is ca. 34.1 kJ mol^{-1} more thermodynamically favorable for X = B(NMeCH)$_2$ than for X = Me (see ESI). This, in turn, is consistent with the significantly greater intrinsic strength of M−B over M−C bonds as determined by Hartwig and Nolan.[67]

EXPERIMENTAL SECTION

Synthetic Procedures. *General Methods and Instrumentation.* All manipulations were carried out using standard Schlenk line or drybox techniques under an atmosphere of argon. Solvents were degassed with dinitrogen and dried by passing through a column of the appropriate drying agent.[68] Tetrahydrofuran was refluxed over sodium/benzophenone and distilled. NMR spectra were measured in benzene-d_6 or toluene-d_8, which had been dried over sodium or potassium, distilled under reduced pressure and stored under argon in a Teflon valve ampule. Photolysis experiments were carried out using a low pressure mercury vapor lamp (1 kW) with samples contained within Schlenk flasks or NMR tubes. Chromatographic separations were carried out with silica gel 60 (63−200 μm particle size). Thin layer chromatography was performed on silica plates 60-F$_{254}$ (12 μm paricle size) containing fluorescence indication for the visualization of UV absorbing compounds. NMR samples were prepared under argon in 5 mm Wilmad 507-PP tubes fitted with J. Young Teflon valves. ^{1}H, ^{13}C{^{1}H}, ^{11}B{^{1}H} and ^{31}P{^{1}H} NMR spectra were recorded on a Varian Mercury-VX-300, a Bruker Mercury Avance III HD NanoBay 400 or a Bruker Avance III 500 spectrometer at ambient temperature unless otherwise stated, and referenced internally to residual protio-solvent (^{1}H) or solvent (^{13}C) resonances, and are reported in ppm relative to tetramethylsilane (δ = 0 ppm). ^{11}B{^{1}H} NMR and ^{31}P{^{1}H} NMR spectra were referenced to external Et$_2$O·BF$_3$ or 85% H$_3$PO$_4$, respectively. Assignments were confirmed using two-dimensional HSQC correlation experiments. Chemical shifts are quoted in ppm. Solid state and solution phase infrared spectra were measured on a Nicolet iS5 FT-IR spectrometer using air sealed KBr-discs or NaCl-cells. Electron impact mass spectra of neutral compounds were measured using a Waters GC TOF mass spectrometer. Elemental analyses were carried out at London Metropolitan University or at University of Leipzig.

Starting Materials. (THF)$_2$Li{B(NDippCH)$_2$} (**1**),[19] (OC)$_5$Mn{C(O)OEt} (**6**),[69] (OC)$_5$Re{C(O)OMe} (**9**),[70] CpFe(CO)$_2${C(O)OEt} (**12**),[71] CpFe(CO)$_2${C(S)OMe} (**15**),[72] Na[Co(CO)$_4$],[73] Mes$_2$BBr,[74] Co(CO)$_3$(PPh$_3$){C(O)OEt}[53] were synthesized according to literature procedures. [CpFe(^{13}CO)$_2$]$_2$[75] Na[CpFe(^{13}CO)$_2$][5] were synthesized following procedures for the unlabeled materials.

[{(HCDippN)$_2$B}Mn(THF)(μ-Br)]$_2$ (2). A solution of **1** (200 mg, 0.370 mmol) in THF (10 mL) was added to a stirred suspension of MnBr$_2$ (80 mg, 0.370 mmol) in THF (10 mL) at −78 °C. The resulting solution was slowly warmed to 0 °C over a period of 5 h whereupon volatiles were removed in vacuo. The solid was extracted into pentane (2 × 8 mL) and filtered. The extract was concentrated to ca. 10 mL and stored at −30 °C overnight to give pale pink crystals of **2** (106 mg, 0.178 mmol, 48%). The ^{1}H NMR spectrum of **2** is silent in the range δ_H = −200 to +200 ppm. Magnetic moment (μ_B, Evans method, C$_6$D$_6$) 6.8(2) BM. IR (Nujol): 1598 (s), 1377 (s), 1259 (s), 1094 (s), 1020 (s), 871 (m), 700 (s). Elemental analysis found: C 60.50%, H 7.33%, N 4.85%, calculated for C$_{60}$H$_{88}$B$_2$Br$_2$Mn$_2$N$_4$O$_2$ C 60.63%, H 7.46%, N 4.71%.

Fe(CO)$_4${C[OLi(THF)$_3$]B(NDippCH)$_2$} (3). Fe(CO)$_5$ (freshly filtered to remove iron particles, 0.50 mL, 3.71 mmol) was added to a solution of **1** (300 mg, 0.557 mmol) in THF (2 mL). Upon gentle removal of the solvent yellow crystals (mm-size) started to form. The supernatant solution was decanted, and the crystals were washed with hexanes (4 mL) and dried for 5 min in vacuo to give **3** (269 mg, 0.334 mmol, 60%) as yellowish, crystalline power. Further drying led to decomposition. NMR spectra could only be recorded from freshly prepared samples within a few hours since **3** reversibly regenerates the starting material. ^{1}H NMR (C$_6$D$_6$, 299.9 MHz, 293 K): δ 1.25 (12 H, d, ^3J = 7.2 Hz, CH*Me*$_2$), 1.32 [12 H, s, br, O(CH$_2$*CH*$_2$)$_2$], 1.49 (12 H, d, ^3J = 7.2 Hz, CH*Me*$_2$), 3.35 [12 H, s, br, O(*CH*$_2$CH$_2$)$_2$], 3.59 (4 H, septet, ^3J = 6.3 Hz, *CH*Me$_2$), 6.07 (2 H, s, NCH), 7.11−7.19 (6 H, m, C$_6$*H*$_3$^{i}Pr$_2$). ^{13}C{^{1}H} NMR (C$_6$D$_6$, APT, 125.7 MHz, 293 K): δ 23.8 (CH$_3$), 25.4 (O(CH$_2$CH$_2$)$_2$), 26.0 (CH$_3$), 28.4 (CH), 68.2 (O-(CH$_2$CH$_2$)$_2$), 118.7 (CH, NCH), 123.6 (CH-aryl), 127.7 (CH-aryl), 139.1 (C-aryl), 146.9 (C-aryl), 220.2 (CO), not observed C-carbene. ^{11}B{^{1}H} NMR (C$_6$D$_6$, 96.2 MHz, 293 K): δ 21.3 ($\omega_{1/2}$ = 545 Hz). IR (KBr-disc): ν(CO) 2011, 1931, 1906, 1851 cm^{-1}. Elemental analysis

dx.doi.org/10.1021/ja508979x | J. Am. Chem. Soc. 2014, 136, 15730−15741

found: C 63.74, H 7.75, N 3.77%, calculated for $C_{43}H_{60}BFeLiN_2O_8$ C 64.03, H 7.50, N 3.47.

$Cr(CO)_5${C[OLi(THF)$_2$]B(NDippCH)$_2$} (4). $Cr(CO)_6$ (freshly sublimed, 140 mg, 0.636 mmol) and **1** (350 mg, 0.650 mmol) were dissolved in THF (3 mL) and stirred at ambient temperature for 30 min. The solution turned to orange-red. The solvent was reduced to 0.5 mL and the solution was diluted with hexanes (5 mL). Orange microcrystals formed at −25 °C overnight, which were dried in vacuo to a constant proportion of coordinated THF (commonly 6 h) to give **3** (434 mg, 0.572 mmol, 90%). ^{1}H NMR (C_6D_6, 299.9 MHz, 293 K): δ 1.22 (12 H, d, ^3J = 6.3 Hz, CHMe_2), 1.31 [8 H, s, br, O(CH_2CH_2)$_2$], 1.48 (12 H, d, ^3J = 6.3 Hz, CHMe_2), 3.29 [8 H, s, br, O(CH_2CH_2)$_2$], 3.58 (4 H, septet, ^3J = 6.9 Hz, CHMe$_2$), 6.09 (2 H, s, NCH), 7.15−7.18 (6 H, m, $C_6H_3{}^iPr_2$). ^{13}C{^{1}H} NMR (C_6D_6, APT, 125.7 MHz, 293 K): δ 23.3 (CH_3), 25.3 (O(CH_2CH_2)$_2$), 26.6 (CH_3), 28.5 (CH), 68.5 (O(CH_2CH_2)$_2$), 118.7 (CH, NCH), 123.5 (CH-aryl), 127.3 (CH-aryl), 139.3 (C-aryl), 146.6 (C-aryl), 222.2 (4 *cis*-CO), 228.1 (*trans*-CO), not observed C-carbene. ^{11}B{^{1}H} NMR (C_6D_6, 96.2 MHz, 293 K): δ 21.6 ($\omega_{1/2}$ = 497 Hz). IR (KBr-disc): ν(CO) 2030, 1982, 1955, 1910, 1851 cm^{-1}. Elemental analysis found: C 63.10, H 7.08, N 3.60%, calculated for $C_{40}H_{52}BCrLiN_2O_8$ C 63.33, H 6.91, N 3.69.

$(OC)_5$Cr{C(OEt)B(NDippCH)$_2$} (5). Complex **4** (400 mg, 0.523 mmol) was dissolved in DCM (5 mL) and the orange-red solution was cooled to −78 °C. [Et_3O][BF_4] (150 mg, 0.790 mmol) was added and the solution was allowed to warm to ambient temperature within 2 h. The solvent was evaporated in vacuo. Trace amounts of volatile impurities were removed by dissolution in pentane (3 mL) and evaporation in vacuo. The resulting deep red powder was dissolved in pentane (10 mL) and filtered. The filtrate was reduced to a volume of 2 mL. Deep red crystals of **5** (suitable for X-ray crystallography) were obtained at −35 °C within 5 d (181 mg, 0.284 mmol, 54%). ^{1}H NMR (C_6D_6, 299.9 MHz, 293 K): δ 0.74 (3 H, t, ^3J = 7.2 Hz, CH_2CH_3), 1.10 (12 H, d, ^3J = 7.2 Hz, CHMe_2), 1.28 (12 H, d, ^3J = 7.2 Hz, CHMe_2), 3.17 (4 H, septet, ^3J = 7.2 Hz, CHMe$_2$), 4.80 (2 H, q, ^3J = 7.2 Hz, CH_2CH_3), 5.99 (2 H, s, NCH), 7.04−7.18 (6 H, m, $C_6H_3{}^iPr_2$). ^{13}C{^{1}H} NMR (C_6D_6, APT, 125.7 MHz, 293 K): δ 14.6 (CH_2CH_3), 23.4 (CH_3), 26.0 (CH_3), 28.6 (CH), 80.5 (CH_2CH_3), 120.1 (CH, NCH), 123.6 (CH-aryl), 124.1 (CH-aryl), 138.5 (C-aryl), 145.9 (C-aryl), 216.2 (4 *cis*-CO), 225.7 (*trans*-CO), not observed C-carbene. ^{11}B{^{1}H} NMR (C_6D_6, 96.2 MHz, 293 K): δ 23.3 ($\omega_{1/2}$ = 274 Hz). IR (KBr-disc): ν(CO) 2056, 1986, 1948, 1934, 1914 cm^{-1}. Elemental analysis found: C 63.81, H 6.38, N 4.53%, calculated for $C_{34}H_{41}BCrN_2O_6$ C 64.16, H 6.46, N 4.40.

$(OC)_5$Mn{B(NDippCH)$_2$} (8). **1** (500 mg, 0.928 mmol) in THF (10 mL) was added to $(OC)_5$Mn{C(O)OEt} (**6**, 250 mg, 0.933 mmol) in THF (10 mL) and stirred at room temperature for 30 min. Silica gel (two spatulas) was added to the solution and the solvent was removed in vacuo before the air and moisture-stable complex was purified by column chromatography (hexanes). Crystallization from hexanes by slow solvent evaporation yielded colorless crystals of **8** (340 mg, 0.584 mmol, 63%), one of which was suitable for X-ray crystallography. R_f (hexanes) = 0.43. ^{1}H NMR (C_6D_6, 400 MHz, 293 K): δ 1.18 (12 H, d, ^3J = 6.8 Hz, CHMe_2), 1.33 (12 H, d, ^3J = 6.8 Hz, CHMe_2), 3.35 (4 H, septet, ^3J = 6.8 Hz, CHMe$_2$), 6.42 (2 H, s, NCH), 7.11−7.23 (6 H, m, $C_6H_3{}^iPr_2$). ^{13}C{^{1}H} NMR (C_6D_6, APT, 126 MHz, 293 K): δ 23.0 (CH_3), 26.4 (CH_3), 28.1 (CH), 123.6 (CH, NCH), 124.3 (CH-aryl), 128.4 (CH-aryl), 140.3 (C-aryl), 147.2 (C-aryl), 211.1 (*trans*-CO), 212.6 (4 *cis*-CO). ^{11}B{^{1}H} NMR (C_6D_6, 128 MHz, 293 K): δ 33.7 ($\omega_{1/2}$ = 202 Hz). IR (KBr disc): ν(CO) 2093, 1998, 1985, 1976 cm^{-1}. EI MS: 582.2 ([M]$^+$, 9%), 470.2 ([M−4CO]$^+$, 12%), 442.2 ([M−5CO]$^+$, 30%). Elemental analysis found: C 64.32, H 6.31, N 4.84%, calculated for $C_{31}H_{36}BMnN_2O_5$ C 63.93, H 6.23, N 4.81%.

$(OC)_5$Re{C(O)B(NDippCH)$_2$} (10). **1** (140 mg, 0.260 mmol) in THF (10 mL) was added to a solution of $(OC)_5$Re{C(O)OMe} (**9**, 100 mg, 0.260 mmol) in THF (5 mL) at room temperature and stirred for 30 min. Volatiles were then removed in vacuo and the product triturated with hexanes (3 × 5 mL) before being extracted with hexanes. The volume of the solvent was reduced to a minimum and orange crystals of **10** (suitable for X-ray crystallography) were obtained by solvent evaporation over 6 h in air (54 mg, 72.8 μmol, 28%). ^{1}H NMR (C_6D_6, 400 MHz, 293 K): δ 1.14 (12 H, d, ^3J = 6.4 Hz, CHMe_2), 1.43 (12 H, d, ^3J = 6.8 Hz, CHMe_2), 3.40 (4 H, septet, ^3J = 6.8 Hz, CHMe$_2$), 6.02 (2 H, s, NCH), 7.10−7.26 (6 H, m, $C_6H_3{}^iPr_2$). ^{13}C{^{1}H} NMR (C_6D_6, APT, 126 MHz, 293 K): δ 23.4 (CH_3), 26.4 (CH_3), 28.6 (CH), 118.8 (CH, NCH), 123.9 (CH-aryl), 128.0 (CH-aryl), 137.7 (C-aryl), 146.1 (C-aryl), 182.4 (*trans*-CO), 184.4 (*4 cis*-CO), not observed acyl-CO. ^{11}B{^{1}H} NMR (C_6D_6, 128 MHz, 293 K): δ 23.4 ($\omega_{1/2}$ = 395 Hz). IR (KBr disc): ν(CO) 2125, 2071, 2055, 2013, 1992, 1563 cm^{-1}. EI MS: 714.7 ([M−CO]$^+$, 18%), 657.5 ([M−3CO]$^+$, 30%). Elemental analysis found: C 51.63, H 4.80, N 3.65%, calculated for $C_{32}H_{36}BN_2O_6Re$ C 51.82, H 4.89, N 3.78%.

$(OC)_5$Re{B(NDippCH)$_2$} (11). A solution containing $(OC)_5$Re{C(O)B(NDippCH)$_2$} (**10**) in THF (20 mL), prepared via the method outlined above, was heated at 40 °C for 2 d. The solvent was removed in vacuo and the product extracted with hexanes before the air and moisture-stable product was purified by column chromatography (hexanes). Slow solvent evaporation from hexanes yielded colorless crystals of **11** (91 mg, 0.127 mmol, 49%), one of which was suitable for X-ray crystallography. R_f (hexanes) = 0.47. ^{1}H NMR (C_6D_6, 400 MHz, 293 K): δ 1.20 (12 H, d, ^3J = 6.8 Hz, CHMe_2), 1.30 (12 H, d, ^3J = 6.8 Hz, CHMe_2), 3.34 (4 H, septet, ^3J = 6.8 Hz, CHMe$_2$), 6.39 (2 H, s, NCH), 7.12−7.27 (6 H, m, $C_6H_3{}^iPr_2$). ^{13}C{^{1}H} NMR (C_6D_6, APT, 126 MHz, 293 K): δ 23.4 (CH_3), 26.5 (CH_3), 28.6 (CH), 123.4 (CH, NCH), 123.7 (CH-aryl), 128.4 (CH-aryl), 142.0 (C-aryl), 147.3 (C-aryl), 181.9 (*trans*-CO), 185.3 (4 *cis*-CO). ^{11}B{^{1}H} NMR (C_6D_6, 128 MHz, 293 K): δ 32.8 ($\omega_{1/2}$ = 260 Hz). IR (KBr disc): ν(CO) 2114, 2008, 1998, 1970 cm^{-1}. EI MS: 714.8 ([M]$^+$, 5%), 657.5 ([M−2CO]$^+$, 8%). Elemental analysis found: C 52.24, H 5.26, N 3.98%, calculated for $C_{31}H_{36}BN_2O_5Re$ C 52.17, H 5.08, N 3.93%.

$CpFe(CO)_2${C(O)B(NDippCH)$_2$} (13). $CpFe(CO)_2${C(O)-OEt} (**12**, 188 mg, 0.743 mmol, as a stock solution in hexanes) was added to a solution of **1** (400 mg, 0.743 mmol) in THF (10 mL). The resulting orange-red solution was stirred at ambient temperature for 30 min. The solvent was removed in vacuo. The residue was dissolved in hexanes (10 mL) and all volatiles removed to dryness. The orange-red residue was stirred with hexanes (20 mL) for 10 min. Filtration and concentration (to 5 mL) gave an orange, microcrystalline solid, which after isolation is sufficiently clean for further application (**13**, 396 mg, 0.668 mmol, 90%). Analytically pure samples were obtained by passing a concentrated solution of **13** over a layer of silica-gel (4 cm, Et_2O-hexanes, 1:9, v/v). Slow solvent evaporation at ambient temperature gave orange-red prisms of **13** (370 mg, 0.624 mmol, 84%), one of which was suitable for X-ray crystallography. ^{1}H NMR (C_6D_6, 299.9 MHz, 293 K): δ 1.14 (12 H, d, ^3J = 7.2 Hz, CHMe_2), 1.47 (12 H, d, ^3J = 7.2 Hz, CHMe_2), 3.47 (4 H, septet, ^3J = 7.2 Hz, CHMe$_2$), 3.88 (5 H, s, C_5H_5), 6.07 (2 H, s, NCH), 7.10−7.19 (6 H, m, $C_6H_3{}^iPr_2$). ^{13}C{^{1}H} NMR (C_6D_6, APT, 126 MHz, 293 K): δ 23.1 (CH_3), 26.5 (CH_3), 28.6 (CH), 86.5 (C_5H_5), 118.3 (CH, NCH), 123.7 (CH-aryl), 128.06 (CH-aryl), 137.9 (C-aryl), 146.4 (C-aryl), 214.8 (CO), not observed acyl-CO. ^{11}B{^{1}H} NMR (C_6D_6, 96.2 MHz, 293 K): δ 19.6 ($\omega_{1/2}$ = 267 Hz). IR (KBr disc): ν(CO) 2001, 1940, 1610 cm^{-1}. EI MS: 564.0 ([M−CO]$^+$, 5%), 636.0 ([M−2CO]$^+$, 10%, 508.0 [M−3CO]$^+$ 80%). Elemental analysis: found: C 68.40, H 7.19, N 4.65%, calculated for $C_{34}H_{41}BFeN_2O_3$ C 68.94, H 6.98, N 4.73%.

$CpFe(CO)_2${B(NDippCH)$_2$} (14). Thermolysis. $CpFe(CO)_2${C(O)B(NDippCH)$_2$} (**13**, 200 mg, 0.338 mmol) was dissolved in *m*-xylene (3 mL). The orange solution was heated to reflux for 12 h (bp. 140 °C) with a change of the color to deep red. The solvent was removed in vacuo. The residue was dissolved in pentane (8 mL), and silica-gel (two spatulas) was added. The solvent was removed until complete dryness, and the resulting powder was loaded onto a column. Column chromatography [hexanes (50 mL), then elution with toluene] gave **14** (152 mg, 0.270 mmol, 80%). R_f (toluene) = 0.64. Photolysis. $CpFe(CO)_2${C(O)B(NDippCH)$_2$} (**13**, 200 mg, 0.338 mmol) was dissolved in benzene (3 mL). The orange solution was irradiated for 30 min with a change of the color to deep red. The workup as stated above gave **14** (112 mg, 0.199 mmol, 59%). Slow solvent evaporation from solutions of **14** in heptanes gave large yellow prisms suitable for X-ray crystallography. ^{1}H NMR (C_6D_6, 299.9 MHz, 293 K): δ 1.21 (12 H, d, ^3J = 6.9 Hz, CHMe_2), 1.34 (12 H, d, ^3J = 6.9

dx.doi.org/10.1021/ja508979x | J. Am. Chem. Soc. 2014, 136, 15730−15741

Hz, CH*Me*$_2$), 3.44 (4 H, septet, ^3J = 7.2 Hz, C*H*Me$_2$), 4.07 (5 H, s, C_5H_5), 6.43 (2 H, s, NCH), 7.15−7.27 (6 H, m, $C_6H_3{}^iPr_2$). $^{13}C\{^1H\}$ NMR (C_6D_6, APT, 126 MHz, 293 K): δ 23.2 (CH_3), 26.6 (CH_3), 28.6 (CH), 82.7 (C_5H_5), 123.5 (CH, NCH), 123.7 (CH-aryl), 127.8 (CH-aryl), 142.3 (C-aryl), 147.2 (C-aryl), 215.5 (CO). $^{11}B\{^1H\}$ NMR (C_6D_6, 96.2 MHz, 293 K): δ 35.5 ($\omega_{1/2}$ = 203 Hz). IR (KBr disc): ν(CO) 1992, 1932 cm^{-1}. EI MS: 508.2 ([M−2CO]$^+$, 30%). Elemental analysis found: C 69.41, H 7.21, N 4.80%, calculated for $C_{33}H_{41}BFeN_2O_2$ C 70.23, H 7.32, N 4.96%.

CpFe(CO)(CS){C(O)B(NDippCH)$_2$} (16). CpFe(CO)$_2${C(S)OMe} (**15**, 164 mg, 0.743 mmol, as a stock solution in hexanes) was added to a solution of **1** (400 mg, 0.743 mmol) in THF (10 mL). The resulting orange-red solution was stirred at ambient temperature for 5 min. The solvent was removed in vacuo. The residue was dissolved in hexanes (10 mL) and all volatiles removed to dryness. The residue was extracted with hexanes (20 mL), the solution was filtered and concentrated to 3 mL. At −35 °C orange prisms formed within 3−4 h, which were isolated and only shortly dried in vacuo to avoid solvent loss from the lattice. Orange crystals obtained from this procedure were suitable for X-ray crystallography and were found to contain half a molecule of *n*-hexane per fomular unit of the complex **16** according to the formulation CpFe(CO)(CS){C(O)B(NDippCH)$_2$}·(C_6H_{14})$_{0.5}$ (**16**·(C_6H_{14})$_{0.5}$, 361 mg, 0.558 mmol, 76%). The crystals can be handled at ambient temperature but were kept at −78 °C for long-term storage. In solution (even in aliphatic hydrocarbons) **16** decomposes unselectively at ambient temperature within 1−2 d. ^1H NMR (C_6D_6, 400 MHz, 293 K): lattice *n*-hexane omitted for clarity, δ 1.16 (12 H, t, apparent, ^3J = 5.6 Hz, CH*Me*$_2$), 1.47 (6 H, d, ^3J = 5.6 Hz, CH*Me*$_2$), 1.52 (6 H, d, ^3J = 5.6 Hz, CH*Me*$_2$), 3.53 (2 H, septet, ^3J = 5.6 Hz, C*H*Me$_2$), 3.57 (2 H, septet, ^3J = 5.6 Hz, C*H*Me$_2$), 4.00 (5 H, s, C_5H_5), 6.10 (2 H, s, NCH), 7.11−7.17 (6 H, m, $C_6H_3{}^iPr_2$). $^{13}C\{^1H\}$ NMR (C_6D_6, APT, 126 MHz, 293 K): δ 23.1, 23.5, 26.6, 26.7 (4 CH_3), 28.6, 28.7 (CH), 89.3 (C_5H_5), 118.4 (CH, NCH), 123.7, 123.9, 128.3 (3 CH-aryl), 138.1, 146.5, 146,8 (3 C-aryl), 215.1 (CO), 321.5 (CS), not observed acyl-CO. $^{11}B\{^1H\}$ NMR (C_6D_6, 128 MHz, 293 K): δ 19.7 ($\omega_{1/2}$ = 275 Hz). IR (KBr disc): ν(CO) 1995, 1626 cm^{-1}, ν(CS) 1275 cm^{-1}. Elemental analysis found: C 68.45, H 6.83, N 4.28%, calculated for $C_{37}H_{44}BFeN_2O_2S$ C 68.63, H 6.85, N 4.33%.

CpFe(^{13}CO)$_2${C(O)OEt} (12-$^{13}C_2$). Manipulations should be carried out as rapidly as possible since the product is subject to rearrangement. Na[CpFe(^{13}CO)$_2$] (200 mg, 0.990 mmol) was dissolved in THF (5 mL,) and ClC(O)OEt (0.50 mL, 2.627 mmol) was added. The solution was stirred for 2 min at ambient temperature and volatile components were removed in vacuo. The residue was dissolved in hexanes (4 mL), and the solvent was evaporated in vacuo. The red oil obtained was dissolved in hexanes (15 mL) and chilled at −25 °C for 30 min, upon which a small amount of deep red crystals, [CpFe(^{13}CO)$_2$]$_2$, was formed. After filtration the solution was diluted to a predefined volume and immediately used as a stock solution for further manipulations (**12**-$^{13}C_2$, 182 mg, 73%).

CpFe(^{13}CO)$_2${C(O)B(NDippCH)$_2$}(**13**-$^{13}C_2$) and CpFe(^{13}CO)(CO){B(NDippCH)$_2$} (**14**-^{13}C) were prepared as stated for the unlabeled compounds **13** and **14**. The synthesis of compound **14**-^{13}C included both thermal and photolytic rearrangement. The labeled compounds may be handled at ambient temperature, at which they were found to be stable toward rearrangements. The ^1H and $^{11}B\{^1H\}$ NMR spectra of the unlabeled and labeled compounds are identical. For representative IR spectra of compounds **12**-$^{13}C_2$, **13**-$^{13}C_2$ and **14**-^{13}C, see the Supporting Information.

{(OC)$_3$Co}$_3$(μ_3-COBMes$_2$) (20). Na[Co(CO)$_4$] (800 mg, 4.124 mmol) was suspended in toluene (5 mL) and Mes$_2$BBr (452 mg, 1.375 mmol) in toluene (5 mL) was added. The mixture was stirred at 45 °C for 4 d with a continuous change in color to deep purple. The solvent was removed in vacuo and the residue extracted with hexanes (30 mL) and filtered. Concentration of the filtrate (5 mL) and cooling to −25 °C overnight gave deep purple crystals (suitable for X-ray crystallography) of **20** (339 mg, 0.4813 mmol, 35%). ^1H NMR (C_6D_6, 400 MHz, 293 K): δ 2.09 (6 H, s, *para*-CH_3), 3.23 (12 H, s, *ortho*-CH_3), 6.70 (4 H, s, aryl-CH). $^{13}C\{^1H\}$ NMR (C_6D_6, APT, 126 MHz, 293 K): δ 21.2 (CH_3), 23.7 (CH_3), 129.6 (aryl-CH), 134.5 (br, *ipso*-C BMes$_2$), 140.8 (C-aryl), 142.6 (C-aryl), not observed μ^3-C. $^{11}B\{^1H\}$ NMR (C_6D_6, 128 MHz, 293 K): δ 50.4 ($\omega_{1/2}$ = 829 Hz). IR (KBr disc): ν(CO) 2100, 2047, 2036, 2020, 2009, 1954 cm^{-1}. Elemental analysis found: C 47.45, H 3.09%, calculated for $C_{28}H_{22}BCo_3O_{10}$, C 47.63, H 3.14%.

Co(CO)$_3$(PPh$_3$){B(NDippCH)$_2$} (22). A solution of **1** (500 mg, 0.928 mmol) in THF (20 mL) was slowly added to Co(CO)$_3$(PPh$_3$)-{C(O)OEt} (**21**, 488 mg, 1.02 mmol) in THF (20 mL) at precisely −35 °C and stirred for exactly 6 h. The intense yellow solution was slowly (2 h) brought to room temperature and PPh$_3$ (243 mg, 928 μmol) was added. The solution was left to stir for 24 h before the solvent was removed in vacuo. The air and moisture stable product was purified by column chromatography (400 mL hexanes, then toluene:hexanes, 1:7, v/v). Crystallization from hexanes by slow solvent evaporation yielded colorless crystals (120 mg, 150 mmol, 16%), suitable for X-ray crystallography. R_f (hexanes) = 0.34. ^1H NMR (C_6D_6, 400 MHz, 293 K): δ 1.24 (12 H, d, ^3J = 6.6 Hz, CH*Me*$_2$), 1.41 (12 H, d, ^3J = 6.6 Hz, CH*Me*$_2$), 3.57 (4 H, septet, ^3J = 6.9 Hz, C*H*Me$_2$), 6.58 (2 H, s, NCH), 6.91 (6 H, m, CH, PPh$_3$), 7.20−7.30 (m, 6 H, aryl-CH), 7.38 (9 H, m, CH, PPh$_3$). $^{13}C\{^1H\}$ NMR (C_6D_6, APT, 126 MHz, 293 K): δ 23.2 (CH_3), 26.7 (CH_3), 28.7 (CH), 123.7 (CH-aryl), 123.7 (CH, NCH), 127.9 (CH-aryl), 129.0 (CH, d, J_{CP} = 10.7 Hz, PPh$_3$), 130.3 (*para*-CH, PPh$_3$), 133.8 (CH, d, J_{CP} = 10.7 Hz, PPh$_3$), 135.2 (*ipso*-C, d, $^1J_{CP}$ = 44.3 Hz, PPh$_3$), 141.2 (C-aryl), 147.8 (C-aryl), 200.8 (CO, d, $^2J_{CP}$ = 15.3 Hz). $^{11}B\{^1H\}$ NMR (C_6D_6, 128 MHz, 293 K): δ 31.9 ($\omega_{1/2}$ = 412 Hz). $^{31}P\{^1H\}$ NMR (C_6D_6, 162 MHz, 293 K): δ 57.7. IR (KBr disc): ν(CO) 2026, 1962, 1928 cm^{-1}. EI MS: 736.3 ([M−2CO]$^+$, 5%), 708.3 ([M−3CO]$^+$, 5%). Elemental analysis found: C 71.52, H 6.13, N 3.87%, calculated for $C_{47}H_{51}BCoN_2O_3P$, C 71.22, H 6.49, N 3.53%.

■ ASSOCIATED CONTENT

Supporting Information

Experimental data relating to the ^{13}C-isotopic labeling study, crystallographic data including all CIFs (CCDC reference numbers 1020346−1020355), details of DFT calculations. This material is available free of charge via the Internet at http://pubs.acs.org.

■ AUTHOR INFORMATION

Corresponding Authors

rene.frank@chem.ox.ac.uk
michael.mingos@seh.ox.ac.uk
simon.aldridge@chem.ox.ac.uk

Notes

The authors declare no competing financial interest.

■ ACKNOWLEDGMENTS

Dr. Nick Rees is thanked for technical support with VT-NMR measurements. This work was generously supported by the Alexander von Humboldt Foundation (postdoctoral grant to René Frank). We also acknowledge the EPSRC NMSF, Swansea University.

■ REFERENCES

(1) Miyaura, N.; Suzuki, A. *Chem. Rev.* **1995**, *95*, 2457−2483.
(2) Suzuki, A. *J. Organomet. Chem.* **1999**, *576*, 147−168.
(3) Fe, Ru, W: Waltz, K. M.; Hartwig, J. F. *J. Am. Chem. Soc.* **2000**, *122*, 11358−11369.
(4) Mn, Fe, Re: Waltz, K. M.; He, X.; Muhoro, C. N.; Hartwig, J. F. *J. Am. Chem. Soc.* **1995**, *117*, 11357−11358.
(5) Mn, Fe, Re: Waltz, K. M.; Muhoro, C. N.; Hartwig, J. F. *Organometallics* **1999**, *18*, 3383−3393.
(6) Männig, D.; Nöth, H. *Angew. Chem., Int. Ed.* **1985**, *24*, 878−879.
(7) Burgess, K.; Ohlmeyer, M. J. *Chem. Rev.* **1991**, *91*, 1179−1191.
(8) Wadepohl, H. *Angew. Chem., Int. Ed.* **1997**, *36*, 2441−2444.

(9) Beletskaya, I.; Pelter, A. *Tetrahedron* **1997**, *53*, 4957−5026.
(10) Han, L. B.; Tanaka, M. *Chem. Commun.* **1999**, 395−402.
(11) Crudden, C. M.; Edwards, D. *Eur. J. Org. Chem.* **2003**, 4695−4712.
(12) Ishiyama, T.; Matsuda, N.; Miyaura, N.; Suzuki, A. *J. Am. Chem. Soc.* **1993**, *115*, 11018−11019.
(13) Iverson, C. N.; Smith, M. R., III *J. Am. Chem. Soc.* **1995**, *117*, 4403.
(14) Iverson, C. N.; Smith, M. R., III *Organometallics* **1996**, *15*, 5155−5165.
(15) Lesley, G.; Nguyen, P.; Taylor, N. J.; Marder, T. B.; Scott, A. J.; Clegg, W.; Norman, N. C. *Organometallics* **1996**, *15*, 5137−5154.
(16) Ishiyama, T.; Matsuda, N.; Murata, M.; Ozawa, F.; Suzuki, A.; Miyaura, N. *Organometallics* **1996**, *15*, 713−720.
(17) Ishiyama, T.; Yamamoto, M.; Miyaura, N. *Chem. Commun.* **1996**, 2073−2074.
(18) Ishiyama, T.; Miyaura, N. *J. Organomet. Chem.* **2000**, *611*, 392−402.
(19) Segawa, Y.; Yamashita, M.; Nozaki, K. *Science* **2006**, *314*, 113−115.
(20) Segawa, Y.; Suzuki, Y.; Yamashita, M.; Nozaki, K. *J. Am. Chem. Soc.* **2008**, *130*, 16069−16079.
(21) Yamashita, M.; Suzuki, Y.; Segawa, Y.; Nozaki, K. *Chem. Lett.* **2008**, *37*, 802−803.
(22) Segawa, Y.; Suzuki, Y.; Yamashita, M.; Nozaki, K. *J. Am. Chem. Soc.* **2009**, *131*, 9600.
(23) Mg: Yamashita, M.; Suzuki, Y.; Segawa, Y.; Nozaki, K. *J. Am. Chem. Soc.* **2007**, *129*, 9570−9571.
(24) Mg, Cu, Zn: Yamashita, M.; Nozaki, K. *Bull. Chem. Soc. Jpn.* **2008**, *81*, 1377−1392.
(25) Al: Dettenrieder, N.; Dietrich, H. M.; Schädle, C.; Maichle-Mössmer, C.; Törnroos, K. W.; Anwander, R. *Angew. Chem., Int. Ed.* **2012**, *51*, 4461−4465.
(26) Al: Dettenrieder, N.; Hollfelder, C. O.; Jende, L. N.; Maichle-Mössmer, C.; Anwander, R. *Organometallics* **2014**, *33*, 1528−1531.
(27) Ga: Dettenrieder, N.; Schädle, C.; Maichle-Mössmer, C.; Sirsch, P.; Anwander, R. *J. Am. Chem. Soc.* **2014**, *136*, 886−889.
(28) Ga, In, Tl: Protchenko, A. V.; Dange, D.; Harmer, J. R.; Tang, C. Y.; Schwarz, A. D.; Kelly, M. J.; Phillips, N.; Tirfoin, R.; Birjkumar, K. H.; Jones, C.; Kaltsoyannis, N.; Mountford, P.; Aldridge, S. *Nat. Chem.* **2014**, *6*, 315−319.
(29) Si, Ge, Sn: Protchenko, A. V.; Birjkumar, K. H.; Dange, D.; Schwarz, A. D.; Vidovic, D.; Jones, C.; Kaltsoyannis, N.; Mountford, P.; Aldridge, S. *J. Am. Chem. Soc.* **2012**, *134*, 6500−6503.
(30) Pb, Cd, Hg: Protchenko, A. V.; Dange, D.; Schwarz, A. D.; Tang, C. Y.; Phillips, N.; Mountford, P.; Jones, C.; Aldridge, S. *Chem. Commun.* **2014**, *50*, 3841−3844.
(31) Saleh, L. M. A.; Birjkumar, K. H.; Protchenko, A. V.; Schwarz, A. D.; Aldridge, S.; Jones, C.; Kaltsoyannis, N.; Mountford, P. *J. Am. Chem. Soc.* **2011**, *133*, 3836−3839.
(32) Li, S.; Cheng, J.; Chen, Y.; Nishiura, M.; Hou, Z. *Angew. Chem., Int. Ed.* **2011**, *50*, 6360−6363.
(33) Cu: Okuno, Y.; Yamashita, M.; Nozaki, K. *Eur. J. Org. Chem.* **2011**, 3951−3958.
(34) Cu: Okuno, Y.; Yamashita, M.; Nozaki, K. *Angew. Chem., Int. Ed.* **2011**, *50*, 920−923.
(35) Cu, Ag, Au: Segawa, Y.; Yamashita, M.; Nozaki, K. *Angew. Chem., Int. Ed.* **2007**, *46*, 6710−6713.
(36) Cu, Zn: Kajiwara, T.; Terabayashi, T.; Yamashita, M.; Nozaki, K. *Angew. Chem., Int. Ed.* **2008**, *47*, 6606−6610.
(37) Ti, Hf; Terabayashi, T.; Kajiwara, T.; Yamashita, M.; Nozaki, K. *J. Am. Chem. Soc.* **2009**, *131*, 14162−14163.
(38) Reactions were carried out at various temperatures in THF with the respective metal compound being suspended or dissolved. Crude mixtures were investigated by $^{11}B\{^{1}H\}$ NMR. Metal precursors studied included: anhydrous halides MX_2 (M = Mn, Fe, Co, Ni; X = Cl, Br); THF-solvates $MCl_2(THF)_{1.5}$ (M = Mn, Fe, Co, Ni); phosphine complexes $MX_2(PPh_3)_2$ (M = Co, Ni; X = Cl, Br), $CoBr_2(PMe_3)_2$, $NiBr_2(PMe_3)_3$; metal amide $Co[N(SiMe_3)_2]_2$; organometallic complexes $Mn(CO)_5Br$, $CpFe(CO)_2Br$, $M(Mes)_2(PMe_2Ph)_2$ (M = Co, Ni, Mes = 2,4,6-$Me_3C_6H_2$), $NiMe_2(PMe_3)_2$.
(39) The electron affinities of Cr^{2+}, Mn^{2+}, Fe^{2+}, Co^{2+} and Ni^{2+} (i.e., the negative of the second ionization energies of the respective metals) are −1591, −1509, −1562, −1648 and −1753 kJ·mol^{-1}: http://www.webelements.com/periodicity/ionisation_energy_2/ (accessed August 31, 2014).
(40) Baker, R. J.; Jones, C.; Platts, J. A. *Dalton Trans.* **2003**, *19*, 3673−3674.
(41) Protchenko, A. V.; Saleh, L. M. A.; Vidovic, D.; Dange, D.; Jones, C.; Mountford, P.; Aldridge, S. *Chem. Commun.* **2010**, *46*, 8546−8548.
(42) Calderazzo, F. *Angew. Chem., Int. Ed.* **1977**, *16*, 299−311.
(43) Kays, D. L.; Aldridge, S. *Struct. Bonding (Berlin, Ger.)* **2008**, *130*, 29−122.
(44) Fe: Hartwig, J. F.; Huber, S. *J. Am. Chem. Soc.* **1993**, *115*, 4908−4909.
(45) Nöth, H.; Schmid, G. *Allg. Prakt. Chem.* **1966**, *17*, 610−618.
(46) Schmid, G. *Angew. Chem., Int. Ed.* **1970**, *9*, 819−830.
(47) Irvine, G. J.; Lesley, M. J. G.; Marder, T. B.; Norman, N. C.; Rice, C. R.; Robins, E. G.; Roper, W. R.; Whittell, G. R.; Wright, L. J. *Chem. Rev.* **1998**, *98*, 2685−2722.
(48) Braunschweig, H.; Dewhurst, R. D.; Schneider, A. *Chem. Rev.* **2010**, *110*, 3924−3957.
(49) Tran, B. L.; Adhikari, D.; Fan, H.; Pink, M.; Mindiola, D. J. *Dalton Trans.* **2010**, 358−360.
(50) Lin, T.-P.; Peters, J. C. *J. Am. Chem. Soc.* **2013**, *135*, 15310−15313.
(51) Dai, C.; Stringer, G.; Corrigan, J. F.; Taylor, N. J.; Marder, T. B.; Norman, N. C. *J. Organomet. Chem.* **1996**, *513*, 273−275.
(52) Adams, C. J.; Baber, R. A.; Batsanov, A. S.; Bramham, G.; Charmant, J. P. H.; Haddow, M. F.; Howard, J. A. K.; Lam, W. H.; Lin, Z.; Marder, T. B.; Norman, N. C.; Orpen, A. G. *Dalton Trans.* **2006**, 1370−1373.
(53) Hieber, W.; Duchatsch, H. *Chem. Ber.* **1965**, *98*, 1744−1748.
(54) Tasi, M.; Palyi, G. *Organometallics* **1985**, *4*, 1523−1528.
(55) Lavigne, F.; Maerten, E.; Alcaraz, G.; Branchadell, V.; Saffron-Merceron, N.; Baceiredo, A. *Angew. Chem., Int. Ed.* **2012**, *51*, 2489−2491.
(56) Krueger, C.; Goddard, R.; Claus, K. H. *Z. Naturforsch., B: Chem. Sci.* **1983**, *38*, 1431−1440.
(57) Mills, O. S.; Redhouse, A. D. *Angew. Chem., Int. Ed.* **1965**, *4*, 1082.
(58) Darensbourg, M. Y.; Darensbourg, D. J. *Inorg. Chem.* **1970**, *9*, 32−39.
(59) For a related (amido)manganese complex, see: Hicks, J.; Jones, C. *Inorg. Chem.* **2013**, *52*, 3900−3907.
(60) For terphenyl systems displaying similar structures, see: Ellison, J. J.; Power, P. P. *J. Organomet. Chem.* **1996**, *526*, 263−267.
(61) Zhu, J.; Lin, Z.; Marder, T. B. *Inorg. Chem.* **2005**, *44*, 9384−9390.
(62) Closson, R. D.; Kozikowski, J.; Coffield, T. H. *J. Org. Chem.* **1957**, *22*, 598.
(63) Hieber, W.; Braun, G.; Beck, W. *Chem. Ber.* **1960**, *93*, 901−908.
(64) King, R. B. *J. Am. Chem. Soc.* **1963**, *85*, 1918−1922.
(65) King, R. B.; Bisnette, M. B. *J. Organomet. Chem.* **1964**, *2*, 15−37.
(66) Braunschweig, H.; Kollmann, C.; Koster, M.; Englert, U.; Müller, M. *Eur. J. Inorg. Chem.* **1999**, 2277−2281.
(67) Rablen, P. R.; Hartwig, J. F.; Nolan, S. P. *J. Am. Chem. Soc.* **1994**, *116*, 4121−4122.
(68) Pangborn, A. B.; Giardello, M. A.; Grubbs, R. H.; Rosen, R. K.; Timmers, F. J. *Organometallics* **1996**, *15*, 1518−1520.
(69) Kruck, T.; Noack, M. *Chem. Ber.* **1964**, *97*, 1693−1703.
(70) Brodie, A. M.; Hulley, G.; Johnson, B. F. G.; Lewis, J. *J. Organomet. Chem.* **1970**, *24*, 201−203.
(71) Cavanaugh, M. D.; Gregg, B. T.; Chiulli, R. J.; Cutler, A. R. *J. Organomet. Chem.* **1997**, *547*, 173−182.
(72) Busetto, L.; Graziani, M.; Belluco, U. *Inorg. Chem.* **1971**, *10*, 78−80.

(73) Gallo, V.; Mastrorilli, P.; Nobile, C. F.; Braunstein, P.; Englert, U. *Dalton Trans.* **2006**, 2342−2349.
(74) Sundararaman, A.; Jäkle, F. *J. Organomet. Chem.* **2003**, *681*, 134−142.
(75) Ruiz, J.; Lacoste, M.; Astruc, D. *J. Am. Chem. Soc.* **1990**, *112*, 5471−5483.